Molecular and Cellular Endocrinology 594 (2024) 112378

Contents lists available at ScienceDirect

Molecular and Cellular Endocrinology

journal homepage: www.elsevier.com/locate/mce

Extragonadal function of follicle-stimulating hormone: Evidence for a role in endothelial physiology and dysfunction

Maria Santa Rocca [a], Micaela Pannella [d], Erva Bayraktar [b,c], Saralea Marino [b,c], Mario Bortolozzi [b,c], Andrea Di Nisio [d,e], Carlo Foresta [d], Alberto Ferlin [a,d,*]

[a] University Hospital of Padua, Unit of Andrology and Reproductive Medicine, Padua, Italy
[b] University of Padua, Department of Physics and Astronomy "G. Galilei", Padua, Italy
[c] Veneto Institute of Molecular Medicine (VIMM), Via Orus 2, 35129, Padua, Italy
[d] University of Padua, Department of Medicine, Padua, Italy
[e] Department of Wellbeing, Nutrition and Sport, Pegaso Telematic University, Centro Direzionale Isola F2, Naples, Italy

ARTICLE INFO

Keywords:
FSH
FSHR
Calcium imaging
Endothelial integrity
VE-Cadherin

ABSTRACT

Aims: Follicle-stimulating hormone (FSH) plays a fundamental role in reproduction stimulating ovarian folliculogenesis, Sertoli cells function and spermatogenesis. However, the recent identification of FSH receptor (FSHR) also in extra-gonadal tissues has suggested that FSH activity may not be limited only to fertility regulation, with conflicting results on the possible role of FSH in endothelial cells. The aim of this study was to investigate FSH role on endothelial function in Human Umbilical Vein Endothelial Cells (HUVECs).

Results: Endothelial Nitric oxide synthase (*eNOS*) expression, eNOS phosphorylation and Nitric Oxide (NO) production resulted increased after the stimulation of HUVEC with recombinant human FSH (rhFSH) at $3.6x10^3$ ng/ml, with increasing Calcium release from intracellular stores. Furthermore, IP_3 production increased after rhFSH stimulation despite PTX treatment and NFAT1 was observed prevalently in nucleus.

We observed a statistical difference between untreated cells and cells stimulated with $0.36x10^3$ ng/ml and between cells stimulated with $0.36x10^3$ ng/ml and cells stimulated with $1.8x10^3$ ng/ml at 4 and 8 h by Wound healing assay, respectively. Furthermore, a higher cellular permeability was observed in stimulated cells, with atypical VE-cadherin distribution, as well as filamentous actin.

Conclusions: Our findings suggest that FSH at high concentrations elicits a signalling that could compromise the endothelial membrane. Indeed, VE-cadherin anomalies may severely affect the endothelial barrier, resulting in an increased membrane permeability. Although NO is an important vasodilatation factor, probably an excessive production could impact on endothelial functionality, partially explaining the increased risk of cardiovascular diseases in menopausal women and men with hypogonadism.

1. Introduction

Follicle-stimulating hormone (FSH) is a glycoprotein hormone produced and released by the anterior pituitary gland in response to gonadotropin-releasing hormone (GnRH) (Kaprara and Huhtaniemi, 2018). It is composed of an α subunit common to luteinizing hormone (LH) and thyroid stimulating hormone (TSH) and a specific β subunit (Pierce and Parsons, 1981) and it plays a fundamental role in reproduction in both sexes by stimulating ovarian folliculogenesis and testicular spermatogenesis (D'Antonio et al., 1999; Oduwole et al., 2018; Santi et al., 2020). Since the FSH receptor (FSHR) expression was considered exclusively gonad-specific, a possible biological role of FSH in other organs was disregarded for many years. However, the recent identification of FSHR also in extragonadal tissues has suggested that FSH activity may not be limited only to fertility regulation (Liu et al., 2017; Robinson et al., 2010; Stilley et al., 2014; Sun et al., 2006). This finding has sparked many groups' interest, opening intriguing hypotheses on novel functional aspects of FSH. However, FSHR extragonadal expression is still under investigation, and consequently, the possible role of FSH in extra-reproductive organs is still relatively unexplored (Chrusciel et al., 2019; Rajendra Kumar, 2014, 2018).

FSHR is a transmembrane protein belonging to the large family of G-

* Corresponding author. Department of Medicine, Unit of Andrology and Reproductive Medicine, University of Padova, Via Giustiniani, 2, 35128, Padova, Italy.
E-mail address: alberto.ferlin@unipd.it (A. Ferlin).

https://doi.org/10.1016/j.mce.2024.112378
Received 11 April 2024; Received in revised form 13 September 2024; Accepted 23 September 2024
Available online 25 September 2024

protein coupled receptor and consisting of three functional domains: an extracellular domain with multiple leucine-rich repeats (LRRs), seven transmembrane helices (7TM) and a C-terminal domain (Dias et al., 2002; Hsu, 2003; Segaloff, 1993; Simoni et al., 1997). Although for several decades the Gαs/adenylyl cyclase/cAMP/PKA pathway has been considered the canonical mechanism by which FSH exerts its activity (Dattatreyamurty et al., 1987; Hunzicker-Dunn and Maizels, 2006), multiple transduction mechanisms induced by FSH have been demonstrated over last years, leading to the activation of different downstream events such as steroidogenesis, proliferation, apoptosis and survival signals (Casarini and Crépieux, 2019). Each of these pathways is modulated by different intracellular effectors, whose activation depends mainly on the tissue and on particular developmental stage of FSH-target cells (Crépieux et al., 2001; Gloaguen et al., 2011). The stimulated FSHR can interact with heterotrimeric G proteins, causing the dissociation of α-subunits consisting of four families (αs, αq, αi, α12/13) and mediating different molecular signalling depending on released α subunit. Additionally, the receptor could interact with other two protein families such as G protein-coupled receptor kinases (GRKs) and arrestins. Therefore, different molecular mechanisms can be switch on depending on the interactors.

Despite endothelium being included in extragonadal tissues expressing FSHR, the possible role of FSH in this tissue is unclear, since the few published studies reported contrasting findings (Stelmaszewska et al., 2016; Stilley et al., 2014; Tan et al., 2021; Tedjawirja et al., 2023). *FSHR* transcript and FSHR protein has been detected in human umbilical vein endothelial cells (HUVEC) in some studies (Stilley et al., 2014; Tan et al., 2021), but not in others (Tedjawirja et al., 2023). Stilley et al. reported positive effects of FSH in tube formation, wound healing, cell migration, cell proliferation, nitric oxide (NO) production, cell survival, and angiogenic processes in HUVEC (Stilley et al., 2014). Still, Stelmaszewska et al. did not confirm these findings.(Stelmaszewska et al., 2016).

Nevertheless, the understanding of possible physiological roles of FSH on endothelium and of pathologically high circulating levels of FSH in endothelium dysfunction is of great relevance (Li et al., 2017). In fact, endothelial dysfunction is a critical event in the development of cardiovascular diseases (CVDs) (Reitsma et al., 2007), and gonadal impairment with high FSH plasma levels (because of the reduced inhibitory effect at the hypothalamic-pituitary level) is a known risk factor for both endothelial dysfunction and CVDs. Both oestrogenic deficiency in females (as observed for example in physiologic and pathologic menopause) and low testosterone (hypogonadism) in males are known CVDs risk factors and are associated with cardiovascular mortality (Maggio and Basaria, 2009; Xiang et al., 2021). Therefore, although sex hormones directly affects the endothelium (Stanhewicz et al., 2018), a possible direct effect of increased levels of FSH cannot be ignored. Interestingly, subclinical forms of hypogonadism characterised by normal circulating levels of sex hormones and high levels of FSH are still associated with CVDs morbidity and mortality, both in the ageing males (Corona et al., 2021) and in young men for example affected by the Klinefelter syndrome (Accardo et al., 2019; Salzano et al., 2016).

The present study aimed to better investigate FSH activity in HUVEC cell line with different functional and molecular studies to clarify whether FSH might have physiological roles on endothelium and, therefore, whether pathologically high FSH levels might impact on endothelial functionality.

2. Materials and methods

2.1. Cell culture and reagents

HUVECs pools (Life Technologies), were plated on 0,1% gelatin (Sigma Aldrich)-coated tissue culture dishes and maintained in phenol red-free basal medium M200 (Life Technologies) containing 10% FBS (Euroclone), 1% Pen/Strep (Gibco), 1% L-glutamine (Gibco) and LSGS growth factors (Life Technologies) at 37 °C with 5% CO2. HUVEC (passages 2–4) were used for cell stimulation studies. Before the stimulation with recombinant human FSH (rhFSH) (Gonal-f 900IU-66μg/1.5 ml, Merck KGaA, Darmstadt, Germany), HUVECs were hormone-deprived using charcoal/dextran-treated Fetal Bovine Serum (FBS) (Gibco) for 16 h before treatment. Concentrations of rhFSH ranging from 0.36 x 10^3 ng/ml (corresponding at 5 IU/ml) to 11 x 10^3 ng/ml (corresponding at 150 IU/ml) were used for stimulations. Although rhFSH concentrations used in this study are very high, however Riccetti et al. found that to induce a FSHR intracellular interactor different from canonical $G_{\alpha s}$,such as β arrestin 2, 278.6 ± 56.9 ng/ml of Gonal-f were necessary (Riccetti et al., 2019). Additionally, the same authors observed that intracellular Ca^{2+} increase was highlighted exclusively when the cells were stimulated with 4 x 10^3 ng/ml of rhFSH (Riccetti et al., 2019).

2.2. RNA isolation and real-time PCR

HUVECs were seeded at 40% confluence in 6 well-plate and transfected after 18h with 10 nM of FSHR (si)RNA (Origene) (#SR301661, Life Technologies) using siTran 2.0 siRNA transfection reagent (OriGENE Inc, TT320001) when it reached the 50% confluency according the manufacturer's protocol. Cells at 80% confluence were used for experiments (about 48 h after transfection). Scrambled siRNA was added to cells not transfected with siFSHR.

Total RNA was extracted using RNeasy Mini Kit (Qiagen, Hilden, Germany). Then, 500 ng of total RNA were reverse transcribed using SuperScript III reverse transcriptase (Life Technologies, Carlsbad, CA, USA) according to manufacturer's protocol. cDNA was used for real-time PCR experiments to measure the amount of FSHR and e-NOS transcripts. Real-time PCR reactions were conducted on StepOne Plus in a final volume of 20 μl. Primers concentration was 500 nM. Since it has been suggested that HUVECs express exclusively *FSHR* mRNA lacking exon 9 (Stilley et al., 2014) and since it has been demonstrated that exons 2 and 3 are necessary for FSH binding and signalling (Mann et al., 2000), we used primers spanning exons 2–3 (FSHR forward, CTCACCAAGCTTCGAGTCATCCAA and FSHR reverse, AAGGTTGGAGAACACATCTGCCTCT) as described from Stilley et al. (2014) and primers spanning exons 9 (forward, TGGACCAGTCATTCTCTCTGA and reverse, CTCTGCTGTAGCTGGACTCAT) to amplify *FSHR*, whilst the primers eNOS forward 5′- CGGCATCACCAGGAAGAAGA -3′ and eNOS reverse 5′-CATGAGCGAGGCGGAGAT -3′ were used to amplify *eNOS*. Changes in gene expression were calculated by the $2^{-\Delta\Delta Ct}$ formula using GAPDH as reference gene.

2.3. NO production

Before the experiment cells were seeded onto 24-well plate (9x10^4 cells/well). After overnight incubation in culture medium cell were starved for 4 h. Then, the cells were treated without (control) and with rhFSH at increasing concentrations for 24h. After the treatment, the plate was shaken for 90 min to generate shear stress in order to activate NO production. Successively, the cells were incubated for 45 min with 5uM of DAF-FMTM diacetate (Invitrogen, Waltham, MA, USA) at 37 °C. The cells were washed in PBS to remove the excess probe. Fresh HUVEC medium was added to cells that were incubated 30 min to allow complete de-esterification of the intracellular diacetates.

Optical density was obtained using BERTHOLD MITHRAS Spectrophotometer using excitation max at 495 nm and fluorescence max at 515.

2.4. Elisa for p-eNOS and IP3

HUVEC cell lysates were used to quantify p-eNOS and Inositol Triphosphate (IP_3) by ELISA kit according to the manufacturer's protocol (ab279779 and ab287832 respectively, Abcam). For IP_3 assay,

cells stimulated with 3,6 x 10^3 ng/ml of rhFSH were pre-treated for 45 min with and without YM-254890 (Gαq inhibitor; AdipoGen Life Sciences) at 30 nM. Briefly, lysates of cells previously treated overnight with rhFSH were pipetted into the wells pre-coated with eNOS and IP_3. In two micro-plate, anti-phospho eNOS (S1177) (used to detect phosphorylated protein) and IP_3 antibodies were added. In the remaining wells of eNOS Elisa Kit, mouse anti-pan-eNOS antibody (antibody detecting different isoforms of NO synthase) was used to detect total eNOS. After washing away unbound antibody, Horseradish Peroxidase (HRP)-conjugated anti-rabbit IgG or HRP-anti-mouse IgG is pipetted into the wells. The wells are again washed and TMB substrate was added to the wells. The optical density was determined using BERTHOLD MITRHAS reader at 450 nm. A standard curve was generated for both assays. Based on this standard curve, linear regression analysis was performed. The amount of p-eNOS Ser1177 and IP3 in the cells was calculated by comparing the OD of the samples to the standard curve.

2.5. Immunofluorescence

Immunofluorescence was used to identify VE-cadherin, NFAT, phalloidin. Cultured cells treated and not with 3,6 x 10^3 ng/ml of rhFSH were fixed with 4% paraformaldehyde (Sigma-Aldrich) in PBS (Euro-Clone), blocked with 1% normal goat serum (Thermo Fisher), 2% bovine serum albumin (Sigma-Aldrich), 0.3% Triton X 100 in PBS for 1h at room temperature, and incubated with the following primary antibodies overnight in PBS with 0.3%Triton X 100, 1% BSA: rabbit anti-VE cadherin (Cellsignaling, 1:400); rabbit anti- NFAT1 (ab2722, Abcam, 1:1000), cells with phalloidin FITC-conjugated secondary antibody (F432,Thermo Fisher, 1:100) were incubated for 1h. Primary immunoreaction was detected with the proper secondary antibody: goat anti-

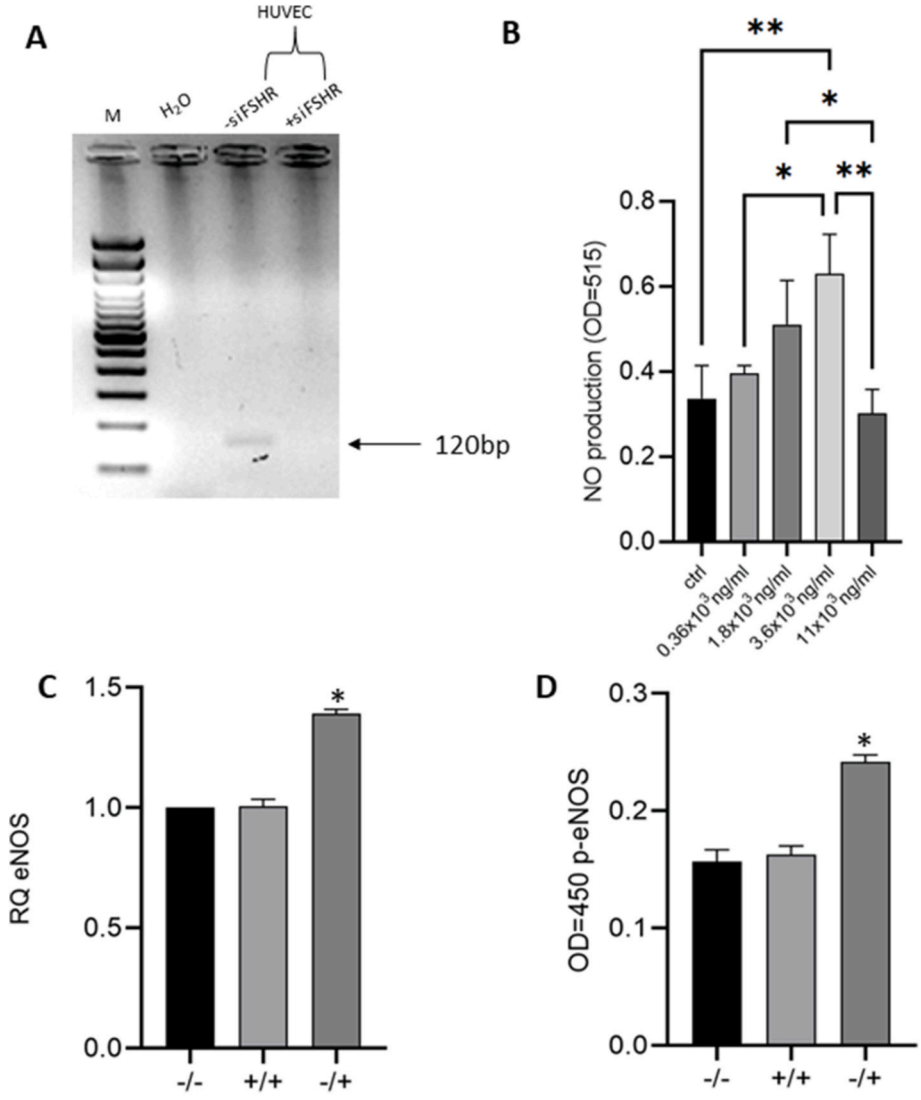

Fig. 1. (A) *FSHR* expression by RT-PCR using primers spanned exons 2 and 3 of *FSHR* gene. A 120 base pairs (bp) PCR product was observed exclusively in cells not transfected with siFSHR.

(B) Production of Nitric oxide (NO) in untreated cells (ctrl) and cells after rhFSH stimulation at concentrations ranging from 0.36 x 10^3 ng/ml to 11 x 10^3 ng/ml. At x-axis there are the different concentrations of rhFSH used. A one-way ANOVA test was performed to calculate the difference among cells stimulated with increasing concentrations of rhFSH. ** = $p < .005$ * = $p \leq 0.05$. Data are the results of three independent biological replicates, with three technical replicates for each, and are represented as mean ± SD. *eNOS* expression (C) and p-eNOS quantification (D) in cells not transfected with siFSHR and untreated cells with rhFSH (−/−), in cells transfected with siFSHR and stimulated with rhFSH (+/+) and in cells not transfected with siFSHR and stimulated with rhFSH (−/+). For cell stimulation, a 3.6 x 10^3 ng/ml dose of rhFSH was used as concentration. Two-tailed Student's t was used to detect the differences between untreated and treated cells (with and without siFSHR transfection). Data are the results of two independent biological replicates, with three technical replicates for each, and are represented as mean ± SD. * = $p < .05$ (C–D).

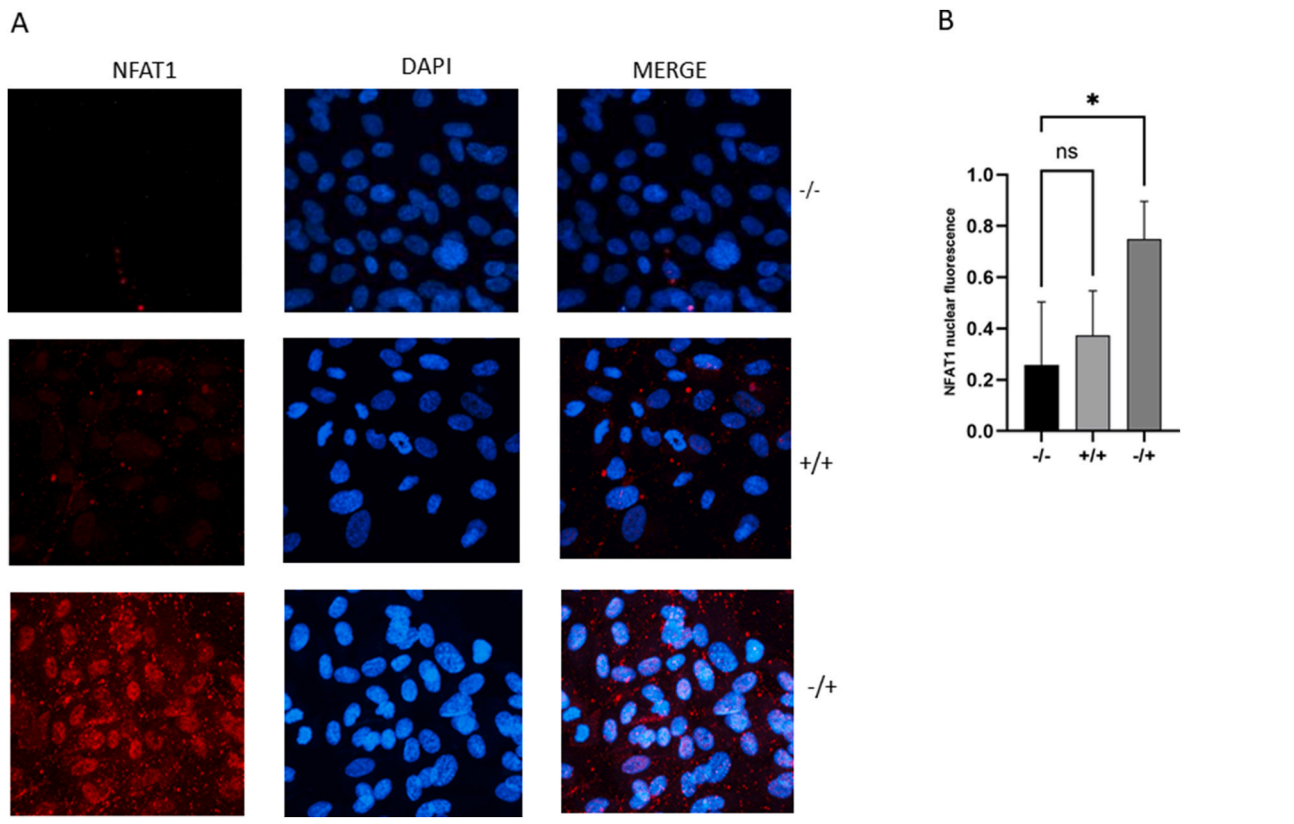

Fig. 2. (A) Immunocytochemical localisation of NFAT1 in untreated cells (−) and cells transfected (+siFSHR) and not transfected (-siFSHR) after rhFSH stimulation at 3.6 x 10^3 ng/ml. Scale bar: 50 μm (40X magnification). (B) Bar graphs showing NFAT1 nuclear localisation cells in not transfected with siFSHR and untreated cells with rhFSH (−/−), in cells transfected with siFSHR and stimulated with rhFSH (+/+) and in cells not transfected with siFSHR and stimulated with rhFSH (−/+). ImageJ software was used to calculate the fluorescence). Data are the results of three independent biological replicates and are represented as mean ± SD.

rabbit IgG (H + L)-Alexa Fluor Plus 647 conjugated (Thermo Fisher). After immunofluorescence staining, cells were counterstained with the nuclear dye DAPI (1 μg/ml in PBS, 0.3% Triton-X 100) for 20 min at RT. Cells were finally washed in PBS and mounted in Mowiol (Sigma-Aldrich). Immunofluorescence was visualized by using laser scanning confocal microscopy (ZEISS LSM 710, ZEISS, Germany).

2.6. Calcium assay

Changes in cytosolic Ca^{2+} levels were monitored in HUVECs loaded with the fluorescent Ca^{2+}-sensitive dye Fluo-4 AM (Molecular Probes, Invitrogen). This method allows to monitor the response of the cells to stimulations by molecules thanks to the cell turning on and simultaneously to see the peaks of calcium flow on the graph.

Briefly, HUVECs were incubated with 2 μM Fluo-4 AM for 20 min at 37 °C and washed with external buffer before fluorescence measurements. Fluo-4 fluorescence was recorded with the same photometric microscope set-up as described for FRET measurements. Excitation time was 50 ms at a frequency of 1 Hz. Excitation wavelength was set to 490 nm (exciter ET470/40 × , dichroic T495LP), and emission of single whole cells was recorded at 535 ± 15 nm (DCLP 505 nm). The fluorescence intensity of Fluo-4 increases upon Ca^{2+} binding. To determine whether Ca^{2+} flux was the result of the opening of Calcium channel or the release of ion from intracellular storage, cells were pre-treated with 1 μg/ml pertussis toxin (PTX; Sigma-Aldrich) for 1 h and 3.6 x 10^3 ng/ml of rhFSH has been added. ROIs (regions of interest) are drawn around randomly selected cells that are obtained from image sequences. MATLAB software was used for the analysis of calcium imaging data.

2.7. Wound healing assay

To investigate cell migration, we used the wound healing assay. HUVEC were seeded onto 24-well plate (9x10^4 cells/well) and incubated in culture medium until they reached a confluent monolayer. When the monolayer was reached the cells were treated without rhFSH and with rhFSHR at different concentration (from 0.36 x 10^3 ng/ml to 11 x 10^3 ng/ml). The day after a scratch wound was created using a 200 μl pipette tip. Cells were treated with rhFSH for 4 and 8 h. Pictures were taken automatically every hour from two different places in the same well. Relative wound density was calculated by Image J Software.

2.8. Tube formation assay

HUVECs (passage 2–4) grown to 70–80% confluency in phenolred-free M200 containing 2% FBS and LSGS growth factors were utilized. Cells were hormone-deprived for 8 h in phenol red-free M200 containing 2% charcoal/dextran-treated FBS and treated overnight with rhFSH (concentrations from 0,36 x 10^3 ng/ml to 11 x 10^3 ng/ml) and without treatment as control. Cells were then trypsinized (Gibco) and suspended in fresh media containing their respective treatments and added to 24 wells previously coated with 95ul of Geltrex (Gibco) and treated without (control) or with rhFSH. The plates were incubated at 37 °C and tube formation was monitored. After 4 and 8 h after seeding, images were captured with a Nikon Digital Sight DS-2Mv camera coupled to a light inverted microscope (40X objective). Endothelial cells sprouting was assessed by counting the number of closed intercellular compartments (closed rings or pro-angiogenic structures) in 5 fields per wells.

Six parameters to define endothelial networks were used: Meshes (areas enclosed by segments or master segments), Junctions (group of dots associated with a bifurcation), Segments (elements delimited by

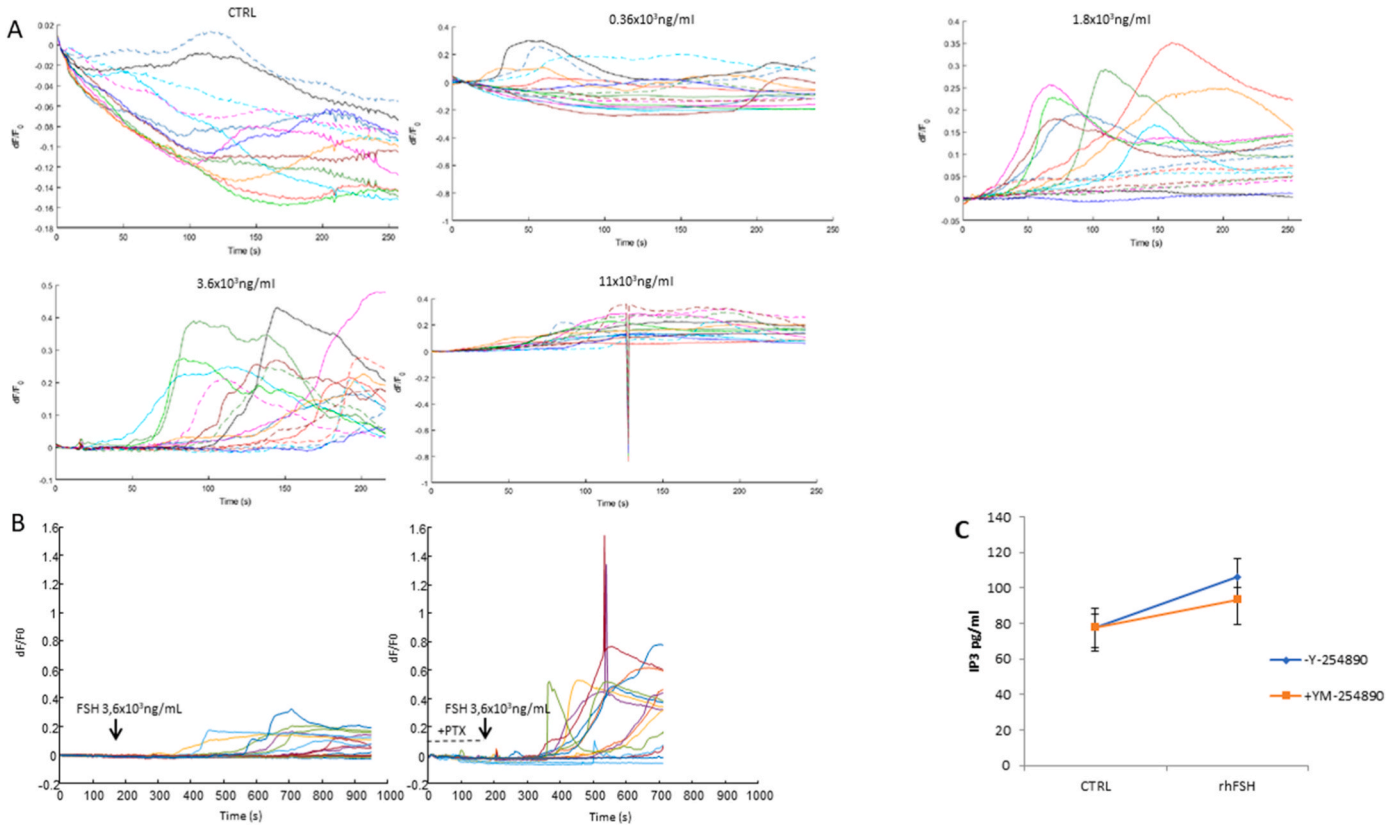

Fig. 3. (A) Intracellular Calcium influx in untreated HUVECs (ctrl) and in HUVECs stimulated with rhFSH at concentrations ranging from 0.36 x 10^3 ng/ml to 11 x 10^3 ng/ml. (B) Calcium imaging data after incubation with PTX and rhFSH stimulation. Colours in A and B figures represent the different cells randomly selected from image sequences and used to calculate fluorescence (dF/F0). dF is the moment-by-moment signal deviation from that baseline; F0 measures the baseline fluorescence. (C) Production of IP_3 in cells untreated (blu) and cells treated with protein $G\alpha_q$ inhibitor (red). IP_3 concentration (pg/ml) has been measured in cells without and with stimulation of rhFSH at 3.6 x 10^3 ng/ml. A four-parameter logistic curve on log-log graph was plotted, with standard concentration on the x-axis and Optical Density (OD) values on the y-axis. Then OD of the samples was measured. The concentration of IP3 in tested samples was calculated by comparing the OD of the samples to the standard curve. The data are represented as means ± SD of three independent technical experiments. * = $p < .05$.

two junctions), Branches (elements delimited by a junction and one extremity), Master Junctions (junctions linking at least three master segments. Optionally, two close master junctions can be fused into a unique master junction) and Master Segments (part of three delimited by two junctions none exclusively implicated with one branch).

ImageJ software (http://image.bio.methods.free.fr/ImageJ/?Gillea-Carpentier&Iang=en) was used for image analysis.

2.9. Permeability assay

Millipore ECM644 was used for permeability assay. The assay was carried out according to the protocol of the Millipore In Vitro Vascular Permeability Assay kit (Catalog#: ECM644; Millipore, Billerica, MA, USA). Briefly, cells (1 × 10^5) were seeded into the culture inserts of permeability chambers that were coated with collagen and incubated at 37 °C until a monolayer was formed. After the cells were starved from serum for 1 h with Hank's balanced salt solution (HBSS), then treated with 3.6 x 10^3 ng/ml rhFSH. Cells were incubated for another 30 min at 37 °C, followed by addition of 75 μl of FITC-Dextran to each insert for 20 min at room temperature (RT), and then 100 μl of the solution in the bottom chamber was transferred to a black 96-well opaque plate. Absorbance at 485 and 535 nm was measured in BERTHOLD MITRHAS reader. Reagent control wells were treated with HBSS only. Blank inserts without plated cells were also included as controls.

2.10. Statistical analysis

All statistics were calculated using SPSS (version 21.0 for Windows; SPSS, Inc., Chicago, IL). The results were expressed as means ± SDs. Data distributions were analysed by Shapiro-Wilk W test for normality, while differences between untreated (−/−) and treated cells (transfected or not with siFSHR, +/+ and −/+ respectively) and between rhFSH treatment groups and negative control were evaluated by Student t-test or one-way ANOVA test where appropriate. Statistical significance was set at $p \leq .05$.

3. Results

RT-PCR showed *FSHR* mRNA expression in HUVEC cells, also confirmed by the lack of *FSHR* transcript after cell transfection with siFSHR (Fig. 1A). This transcript corresponds to the short-length transcript since no amplicon was observed using primers amplifying exon 9 (data not shown).

Nitric oxide (NO) and Ca^{2+} are among the most important mediator of functional activity of endothelial cells, such as vasodilation and angiogenesis. We therefore assessed NO production by shear stress in rhFSH-stimulated cell and found an increased total nitrile mainly at 3.6 x 10^3 ng/ml rhFSH concentration (Fig. 1B). Since NO production depends on *eNOS* gene expression and phosphorylation, we assessed them by RT- PCR (Fig. 1C) and ELISA assay (Fig. 1D) respectively in cells stimulated with rhFSH at 3.6 x 10^3 ng/ml in standard conditions and after silencing of the FSHR through siRNA. 3.6 x 10^3 ng/ml of FSH was used for stimulating since at this concentration a very statistically significant NO production was observed. Both *eNOS* expression and Ser1177 phosphorylation was increased upon FSH stimulation and this effect was mediated by FSHR, as no modification was observed in cells

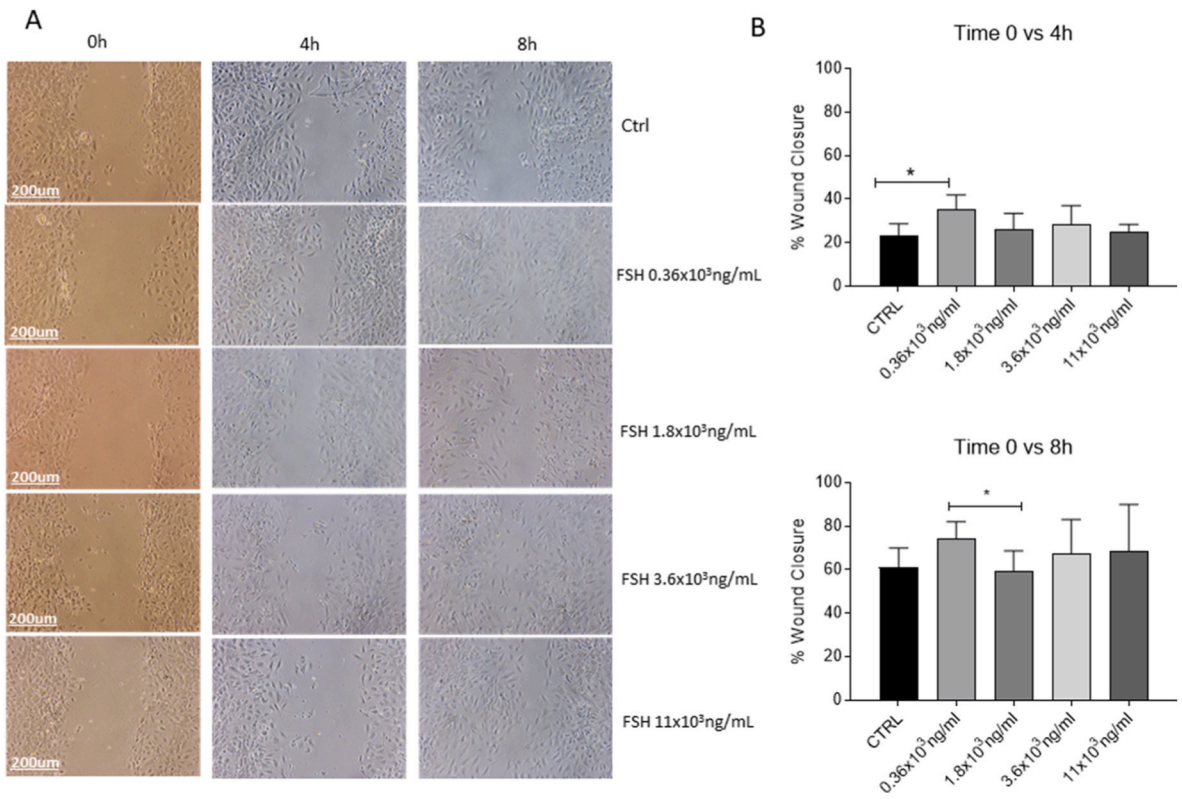

Fig. 4. HUVECs were seeded in 24-well plates and "scratch-wounded" using a universal 200 μl pipette tip. Cells were treated with different concentrations of rhFSH (ranging from 0.36 x 10^3 ng/ml to 11 x 10^3 ng/ml). Microscopy was used to observe and photograph cell migration to the scratch area and calculate the healing area of the wound. Representative photomicrographs were taken at different time points (0h, 4h and 8 h). Scale bar 200 μm (10X magnification) (A). A one-way ANOVA test was performed to calculate the difference among cells stimulated with increasing concentrations of rhFSH. Data are the results of three independent biological replicates, with three technical replicates for each, and are represented as mean ± SD. *: p = .0178 between ctrl and cells stimulated at 0.36x10^3 ng/ml at 4h; *: p = .0489 between 0.36x10^3 ng/ml and cells stimulated at 1.8x10^3 ng/ml at 8h (B).

silenced for FSHR. To further understand the mechanisms underlying *eNOS* induction in FSH-treated cells, we assessed whether FSH stimulated nuclear translocation of NFAT1, a transcriptional activator of *eNOS* gene. Immunofluorescence analysis showed that FSH induced nuclear translocation of NFAT1 and this effect was abolished in cells silenced for FSHR expression (Fig. 2A and B).

We then assessed the possible effect of FSH on intracellular Ca^{2+}, which is necessary in this pathway, being involved in NFAT1 translocation and eNOS phosphorylation. An evident intracellular Ca^{2+} ($[Ca^{2+}]_i$) flux was observed at 1.8 x 10^3 ng/ml and 3.6 x 10^3 ng/ml rhFSH concentration (Fig. 3A). In order to understand the mechanism underlying increased $[Ca^{2+}]_i$, calcium was measured in cells incubated with PTX, that blocking G proteins of G_o/G_i class suppressing intracellular calcium accumulation, and then stimulated with rhFSH (Fig. 3B). Peaks of $[Ca^{2+}]_i$ after rhFSH stimulation were detected despite calcium channel inhibition, suggesting that the increase in $[Ca^{2+}]_i$ was due to release from intracellular calcium stores, which are activated by inositol triphosphate (IP_3) through the phospholipase (PLC) phosphatidylinositol biphosphate (PIP2) pathway after activation of FSHR. Confirming this pathway, we found increased IP_3 production after stimulation with rhFSH (Fig. 3C), but not in cells incubated with a $G\alpha_q$ inhibitor (YM-254890), corroborating the specificity of the signal induced by FSH.

We then assessed the possible functional role of FSH in endothelial cells by wound healing (Fig. 4), tube formation (Fig. 5) using rhFSH concentrations ranging from 0.36 x 10^3 ng/ml to 11 x 10^3 ng/ml and permeability assays (Fig. 6C). We observed, by Wound healing assay, a statistical difference between control and cells stimulated with 0.36x10^3 ng/ml and between cells stimulated with 0.36x10^3 ng/ml and cells stimulated with 1.8x10^3 ng/ml at 4 and 8 h, respectively (Fig. 4B). Additionally, tube formation assay showed the formation of capillary loop like structure in response to increased concentrations of rhFSH (Fig. 5A). The number of meshes, junctions, master segments and master junctions were significantly increased in rhFSH-stimulated cells (Fig. 5B). The effect was mainly evident comparing untreated cells to cells stimulated at 3.6 x 10^3 ng/ml.

Since endothelial integrity is highly dependent on VE-cadherin distribution and function at the endothelial adherens junctions, we determined by immunofluorescence its distribution in cells treated with FSH with/without silenced FSHR.

A jagged VE-cadherin staining after stimulation with rhFSH was observed in cells expressing the FSHR. Specifically, punctate VE-cadherin staining and clear gaps among cells are the result of the loss of the typical cobblestone morphology of endothelial cells. In contrast, cells not stimulated and cells silenced for FSHR showed a narrow borderline (Fig. 6A). Finally, immunofluorescence for filamentous actin (F-actin) by phalloidin probe showed a disorganisation of the protein along stress fibres in cells treated with FSH and the effect was abolished by FSHR silencing (Fig. 6B).

Furthermore, Millipore In Vitro Vascular Permeability Assay kit showed a higher permeability in cells treated with rhFSH, and this effect was abolished in cells silenced for FSHR expression (Fig. 6C).

4. Discussion

We found that FSH might act on HUVEC cells by regulating NO production and release of Ca^{2+} from intracellular stores. At high concentrations, it has functional activity by promoting angiogenesis and detrimental effects on endothelial adherens junctions and permeability. These findings open new perspectives on the possible role of FSH in extragonadal tissues and the pathogenesis of endothelial dysfunction

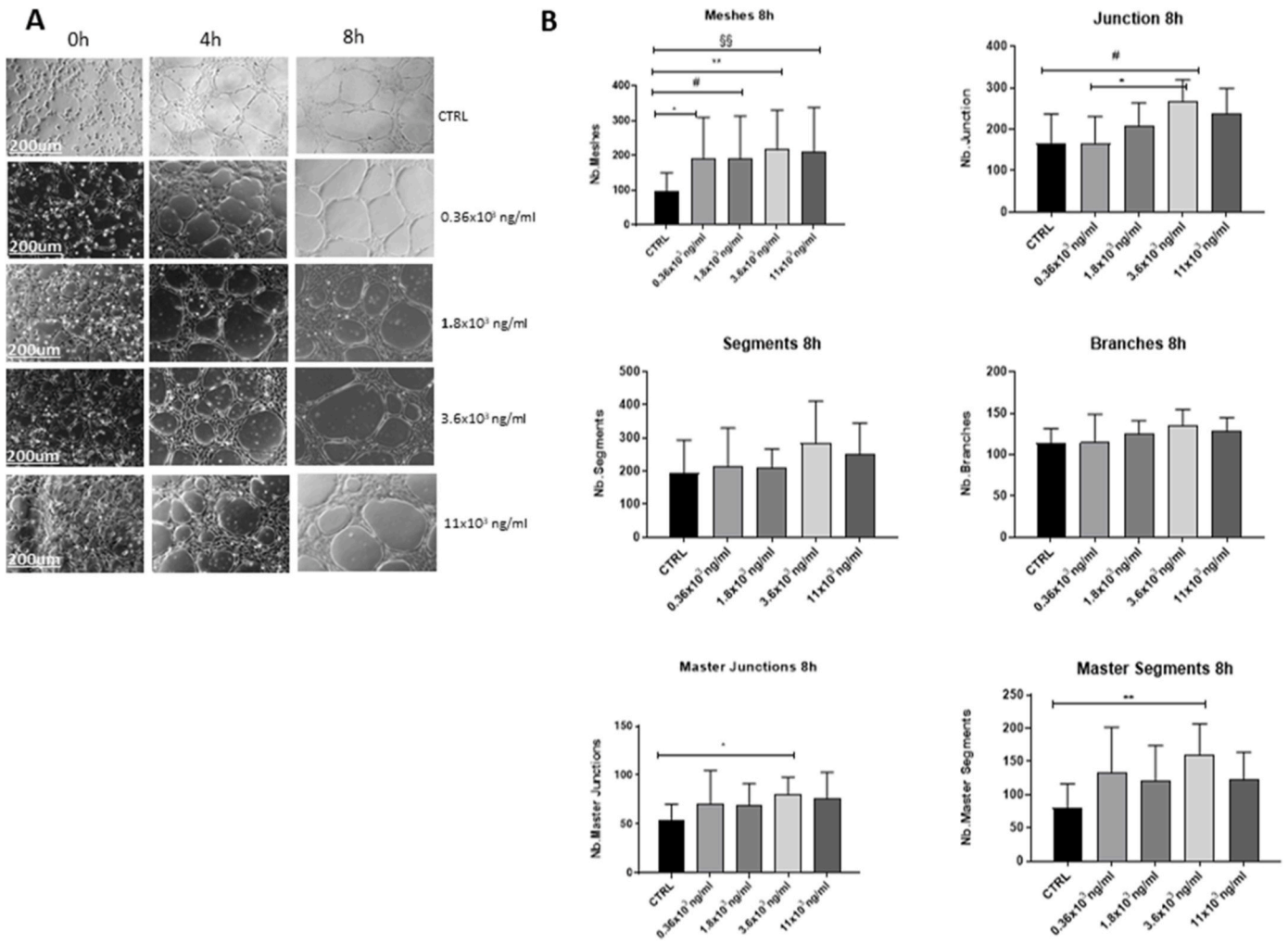

Fig. 5. Tube-forming assay in HUVEC untreated (CTRL) and treated with rhFSH at increasing concentrations (ranging from 0.36 x 10^3 ng/ml to 11 x 10^3 ng/ml). Phase contrast images show the effects of rhFSH on HUVECs. Representative photomicrographs were taken at different time points (0h, 4h and 8 h). Scale bar 200 μm (10X magnification) (A). A one-way ANOVA test was performed, and the graphs show parameters used to evaluate the difference between CTRL and treated cells. Data are the results of three independent biological replicates, with three technical replicates for each, and are represented as mean ± SD. Meshes: *: p = .0145 between ctrl and cells stimulated at 0.36x10^3 ng/ml; #: p = .0295 between ctrl and cells stimulated at 1.8x10^3 ng/ml; **:p = .003 between ctrl and cells stimulated at 3.6x10^3 ng/ml; §§:p = .0099 between ctrl and cells stimulated at 11x10^3 ng/ml; Junctions: #: p = .05 between ctrl and cells stimulated at 3.6x10^3 ng/ml; *: p = .0143 between 0.36x10^3 ng/ml and cells stimulated at 3.6x10^3 ng/ml; Master Junctions: *: p = .0282 between ctrl and cells stimulated at 3.6x10^3 ng/ml; Master Segments: **: p = .0013 between ctrl and cells stimulated at 3.6x10^3 ng/ml (B).

and CDVs in men and women with pathologically high FSH plasma concentrations, such as menopause and primary hypogonadism.

It is well known that CVDs are a leading cause of death and the burden of CVDs has continued to increase drastically in last decades. Considering that most of CVDs risk factors can interfere with endothelial functionality (Widmer and Lerman, 2014), it is believed that most of CVDs arises from endothelial dysfunction (Sun et al., 2020). Endothelium is a monolayer of cells constituting the inner cell layer of blood vessels. It is one of the largest endocrine organ, regulating vascular tone and maintaining vascular homeostasis through several factors, including NO (Krüger-Genge et al., 2019). However, the complex mechanisms underlying endothelial dysfunction are still not completely understood. Vascular ageing is associated with endothelial dysfunction (El Assar et al., 2012) and it is significantly accelerated in the late peri-menopausal period (Moreau and Hildreth, 2014). Although oestrogens have clear roles on endothelium, the decline of endothelial function begins when estrogenic levels are still sufficient to protect endothelium, but FSH levels rise sharply (Moreau, 2018). Similarly, although testosterone has known physiological effects on the cardiovascular system (Di Lodovico et al., 2022), men with subclinical hypogonadism, characterized by normal levels of testosterone with high levels of gonadotropins, are still at increased risk of CVDs and endothelial dysfunction. The findings of our studies, although performed *in vitro* on cell lines, might therefore suggest for a role of pathologically high FSH plasma concentration in the pathogenesis of endothelial dysfunction and CVD risk, at least in these clinical conditions. Interestingly, a study has suggested that FSH could promote atherosclerosis in postmenopausal women (Li et al., 2017).

Interestingly, potential roles of FSH in other extragonadal tissues have been suggested in last years after the identification of FSH receptor in different tissues, such as the bone (Sun et al., 2006) and adipose tissue (Liu et al., 2017). Notably, low bone mass with osteoporosis and visceral adiposity are typical hallmarks of menopause and hypogonadism, and the FSH pathway is under investigation as a potential drug target in these conditions (Zaidi et al., 2018).

We found that the main pathways activated by FSH in HUVEC cells are related to Ca^{2+} and NO. In particular, the increase in $[Ca^{2+}]_i$ depends on the opening of IP_3-sensitive calcium channels in intracellular stores and not on the entry through transmembrane calcium channel. The flux of this ion could determine NO production after FSH

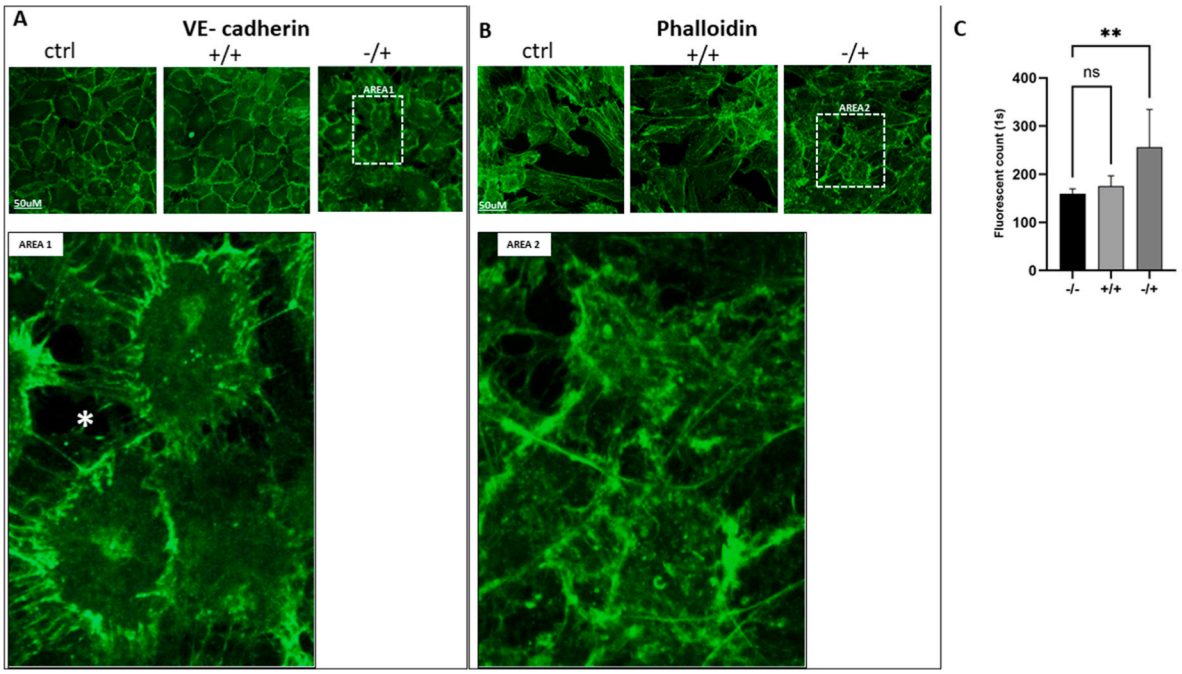

Fig. 6. (A) Immunocytochemical localisation and organisation of VE-cadherin in untreated cells (−/−) and in cells transfected and not with siFSHR after rhFSH stimulation at 3.6 x 10^3 ng/ml rhFSH (+/+ and −/+ respectively). AREA1 in Fig. 6A is a higher magnification of a selected area of −/+ cells and white star indicates the presence of a space between cells. Scale bar:50 μm (40X magnification). (B) Immunocytochemical visualisation of phalloidin in untreated cells (−/−) and in cells transfected and not with siFSHR after rhFSH stimulation at 3.6 x 10^3 ng/ml rhFSH (+/+ and −/+ respectively). AREA2 in Fig. 6B is a higher magnification of a selected area of −/+ cells. Scale bar:50 μm (40X magnification). (C) Fluorescent molecules passing through the endothelial cell monolayer were measured by Millipore ECM644 assay. After hormone treatment of cells seeded onto the collagen-coated inserts, FITC-Dextran, a molecule with high molecular weight, is added on top of the cells, and the extent of permeability is determined by measuring the fluorescence in receveir plate well solution. The bar graph shows the results in untreated cells (−/−) and cells transfected and not transfected with siFSHR after rhFSH stimulation at 3.6 x 10^3 ng/ml dose, +/+ and −/+ respectively. Data are shown as mean ± SD of three independent technical experiments. ** = $p < .05$.

stimulation, through increased nuclear translocation of NFAT1, resulting in eNOS transcription and activation.

Since NO is a known factor involved in the maintaining of vasodilator tone, it is considered a protective factor. However, González et al. (2003) have suggested that this molecule could modify the organization of VE-cadherin complex in mouse (González et al., 2003). VE-cadherin is a transmembrane protein and component of endothelial adherens junctions and it is the most prominent member of the cadherin family expressed in all types of endothelial cells (Bazzoni and Dejana, 2004). A functional VE-cadherin is essential to promote cell-cell adhesion, preserving thus endothelial barrier function (Gavard, 2013). Therefore, altered expression or localisation of this protein may compromise endothelial integrity. After stimulation with rhFSH, we found that adherens junctions were not so tightly together between cells due to an abnormal VE-cadherin distribution. This intriguing finding might suggest that high FSH elicits, through its receptor, a signalling that could compromise the endothelial membrane. It is well-known indeed that the expression and organization of proteins composing tight and adherens junctions are fundamental for the maintaining of endothelial cell homeostasis (Bazzoni and Dejana, 2004). Therefore, anomalies in VE-cadherin may affect severely the endothelial barrier. Furthermore, our study has highlighted an increased membrane permeability after stimulation with high dose of FSH, further suggesting the hypothesis that pathological FSH levels could compromise endothelial integrity.

Although we hope that the findings of our study stimulate the research on the vascular effect of FSH with potential implications for the clinical management of subjects with high FSH, *in vivo* data are needed to confirm our preliminary experimental results. FSH activity is likely amplified *in vitro*. Therefore, clinical studies should be set up to monitor FSH effects on endothelial functionality in subjects with high FSH plasma levels and subjects with normal FSH during FSH treatment.

Data availability

The data underlying this article are available in the article and in its online supplementary material.

Funding

No funding

CRediT authorship contribution statement

Maria Santa Rocca: Writing – review & editing, Writing – original draft, Methodology, Data curation, Conceptualization. **Micaela Pannella:** Writing – review & editing, Methodology. **Erva Bayraktar:** Methodology. **Saralea Marino:** Data curation. **Mario Bortolozzi:** Data curation. **Andrea Di Nisio:** Writing – review & editing, Data curation. **Carlo Foresta:** Writing – review & editing, Conceptualization. **Alberto Ferlin:** Writing – review & editing, Writing – original draft, Data curation, Conceptualization.

Declaration of competing interest

None.

Data availability

all data are in the text

References

Accardo, G., Amoresano Paglionico, V., Di Fraia, R., Cittadini, A., Salzano, A., Esposito, D., De Bellis, A., Pasquali, D., 2019. Management of cardiovascular

complications in Klinefelter syndrome patients. Expet Rev. Endocrinol. Metabol. https://doi.org/10.1080/17446651.2019.1584036.
Bazzoni, G., Dejana, E., 2004. Endothelial cell-to-cell junctions: molecular organization and role in vascular homeostasis. Physiol. Rev. https://doi.org/10.1152/physrev.00035.2003.
Casarini, L., Crépieux, P., 2019. Molecular mechanisms of action of FSH. Front. Endocrinol. https://doi.org/10.3389/fendo.2019.00305.
Chrusciel, M., Ponikwicka-Tyszko, D., Wolczynski, S., Huhtaniemi, I., Rahman, N.A., 2019. Extragonadal FSHR expression and function-is it real? Front. Endocrinol. https://doi.org/10.3389/fendo.2019.00032.
Corona, G., Rastrelli, G., Dicuio, M., Concetti, S., Minnetti, M., Pivonello, R., Isidori, A., Sforza, A., Maggi, M., 2021. Subclinical male hypogonadism. Minerva Endocrinol. https://doi.org/10.23736/S2724-6507.20.03208-3.
Crépieux, P., Marion, S., Martinat, N., Fafeur, V., Vern, Y. Le, Kerboeuf, D., Guillou, F., Reiter, E., 2001. The ERK-dependent signalling is stage-specifically modulated by FSH, during primary Sertoli cell maturation. Oncogene. https://doi.org/10.1038/sj.onc.1204632.
D'Antonio, M., Borrelli, F., Datola, A., Bucci, R., Mascia, M., Polletta, P., Piscitelli, D., Papoian, R., 1999. Biological characterization of recombinant human follicle stimulating hormone isoforms. Hum. Reprod. https://doi.org/10.1093/humrep/14.5.1160.
Dattatreyamurty, B., Figgs, L.W., Reichert, L.E., 1987. Physical and functional association of follitropin receptors with cholera toxin-sensitive guanine nucleotide-binding protein. J. Biol. Chem. https://doi.org/10.1016/s0021-9258(18)60873-7.
Di Lodovico, E., Facondo, P., Delbarba, A., Pezzaioli, L.C., Maffezzoni, F., Cappelli, C., Ferlin, A., 2022. Testosterone, hypogonadism, and heart failure. Circ. Hear. Fail. https://doi.org/10.1161/CIRCHEARTFAILURE.121.008755.
Dias, J.A., Cohen, B.D., Lindau-Shepard, B., Nechamen, C.A., Peterson, A.J., Schmidt, A., 2002. Molecular, structural, and cellular biology of follitropin and follitropin receptor. Vitam. Horm. https://doi.org/10.1016/S0083-6729(02)64008-7.
El Assar, M., Angulo, J., Vallejo, S., Peiró, C., Sánchez-Ferrer, C.F., Rodríguez-Mañas, L., 2012. Mechanisms involved in the aging-induced vascular dysfunction. Front. Physiol. https://doi.org/10.3389/fphys.2012.00132.
Gavard, J., 2013. Endothelial permeability and VE-cadherin A wacky comradeship. Cell Adhes. Migrat. https://doi.org/10.4161/cam.27330.
Gloaguen, P., Crépieux, P., Heitzler, D., Poupon, A., Reiter, E., 2011. Mapping the follicle-stimulating hormone-induced signaling networks. Front. Endocrinol. https://doi.org/10.3389/fendo.2011.00045.
González, D., Herrera, B., Beltrán, A., Otero, K., Quintero, G., Rojas, A., 2003. Nitric oxide disrupts VE-cadherin complex in murine microvascular endothelial cells. Biochem. Biophys. Res. Commun. https://doi.org/10.1016/S0006-291X(03)00546-1.
Hsu, S.Y.T., 2003. New insights into the evolution of the relaxin - LGR signaling system. Trends Endocrinol. Metabol. https://doi.org/10.1016/S1043-2760(03)00106-1.
Hunzicker-Dunn, M., Maizels, E.T., 2006. FSH signaling pathways in immature granulosa cells that regulate target gene expression: branching out from protein kinase A. Cell. Signal. https://doi.org/10.1016/j.cellsig.2006.02.011.
Kaprara, A., Huhtaniemi, I.T., 2018. The hypothalamus-pituitary-gonad axis: tales of mice and men. Metabolism. https://doi.org/10.1016/j.metabol.2017.11.018.
Krüger-Genge, A., Blocki, A., Franke, R.P., Jung, F., 2019. Vascular endothelial cell biology: an update. Int. J. Mol. Sci. https://doi.org/10.3390/ijms20184411.
Li, X., Chen, W., Li, P., Wei, J., Cheng, Y., Liu, P., Yan, Q., Xu, X., Cui, Y., Gu, Z., Simoncini, T., Fu, X., 2017. Follicular stimulating hormone accelerates atherogenesis by increasing endothelial VCAM-1 expression. Theranostics. https://doi.org/10.7150/thno.21216.
Liu, P., Ji, Y., Yuen, T., Rendina-Ruedy, E., DeMambro, V.E., Dhawan, S., Abu-Amer, W., Izadmehr, S., Zhou, B., Shin, A.C., Latif, R., Thangeswaran, P., Gupta, A., Li, J., Shnayder, V., Robinson, S.T., Yu, Y.E., Zhang, X., Yang, F., Lu, P., Zhou, Y., Zhu, L.L., Oberlin, D.J., Davies, T.F., Reagan, M.R., Brown, A., Rajendra Kumar, T., Epstein, S., Iqbal, J., Avadhani, N.G., New, M.I., Molina, H., Van Klinken, J.B., Guo, E.X., Buettner, C., Haider, S., Bian, Z., Sun, L., Rosen, C.J., Zaidi, M., 2017. Blocking FSH induces thermogenic adipose tissue and reduces body fat. Obstet. Gynecol. Surv. https://doi.org/10.1097/01.OGX.0000525900.85600.C2.
Maggio, M., Basaria, S., 2009. Welcoming low testosterone as a cardiovascular risk factor. Int. J. Impot. Res. https://doi.org/10.1038/ijir.2009.25.
Mann, K.I., Liu, X., Dias, J.A., 2000. Deletion of follicle-stimulating hormone (FSH) receptor residues encoded by exon one decreases FSH binding and signaling in the rat. Biol. Reprod. 62. https://doi.org/10.1095/biolreprod62.5.1240.
Moreau, K.L., 2018. Intersection between gonadal function and vascular aging in women. J. Appl. Physiol. https://doi.org/10.1152/japplphysiol.00117.2018.
Moreau, K.L., Hildreth, K.L., 2014. Vascular aging across the menopause transition in healthy women. Adv. Vasc. Med. https://doi.org/10.1155/2014/204390.
Oduwole, O.O., Peltoketo, H., Huhtaniemi, I.T., 2018. Role of follicle-stimulating hormone in spermatogenesis. Front. Endocrinol. https://doi.org/10.3389/fendo.2018.00763.
Pierce, J.G., Parsons, T.F., 1981. Glycoprotein hormones: structure and function. Annu. Rev. Biochem. https://doi.org/10.1146/annurev.bi.50.070181.002341.
Rajendra Kumar, T., 2018. Extragonadal actions of FSH: a critical need for novel genetic models. Endocrinology. https://doi.org/10.1210/en.2017-03118.
Rajendra Kumar, T., 2014. Extragonadal FSH receptor: is it real? Biol. Reprod. https://doi.org/10.1095/biolreprod.114.124222.
Reitsma, S., Slaaf, D.W., Vink, H., Van Zandvoort, M.A.M.J., Oude Egbrink, M.G.A., 2007. The endothelial glycocalyx: composition, functions, and visualization. Pflugers Arch. Eur. J. Physiol. https://doi.org/10.1007/s00424-007-0212-8.
Riccetti, L., Sperduti, S., Lazzaretti, C., Klett, D., De Pascali, F., Paradiso, E., Limoncella, S., Potì, F., Tagliavini, S., Trenti, T., Galano, E., Palmese, A., Satwekar, A., Daolio, J., Nicoli, A., Villani, M.T., Aguzzoli, L., Reiter, E., Simoni, M., Casarini, L., 2019. Glycosylation pattern and in vitro bioactivity of reference follitropin alfa and biosimilars. Front. Endocrinol. 10. https://doi.org/10.3389/fendo.2019.00503.
Robinson, L.J., Tourkova, I., Wang, Y., Sharrow, A.C., Landau, M.S., Yaroslavskiy, B.B., Sun, L., Zaidi, M., Blair, H.C., 2010. FSH-receptor isoforms and FSH-dependent gene transcription in human monocytes and osteoclasts. Biochem. Biophys. Res. Commun. https://doi.org/10.1016/j.bbrc.2010.02.112.
Salzano, A., Arcopinto, M., Marra, A.M., Bobbio, E., Esposito, D., Accardo, G., Giallauria, F., Bossone, E., Vigorito, C., Lenzi, A., Pasquali, D., Isidori, A.M., Cittadini, A., 2016. Management of endocrine disease: Klinefelter syndrome, cardiovascular system, and thromboembolic disease: review of literature and clinical perspectives. Eur. J. Endocrinol. https://doi.org/10.1530/EJE-15-1025.
Santi, D., Crépieux, P., Reiter, E., Spaggiari, G., Brigante, G., Casarini, L., Rochira, V., Simoni, M., 2020. Follicle-stimulating hormone (FSH) action on spermatogenesis: a focus on physiological and therapeutic roles. J. Clin. Med. https://doi.org/10.3390/jcm9041014.
Segaloff, D.L., 1993. The lutropin/choriogonadotropin receptor ... 4 years later. Endocr. Rev. https://doi.org/10.1210/er.14.3.324.
Simoni, M., Gromoll, J., Nieschlag, E., 1997. The follicle-stimulating hormone receptor: biochemistry, molecular biology, physiology, and pathophysiology*. Endocr. Rev. https://doi.org/10.1210/edrv.18.6.0320.
Stanhewicz, A.E., Wenner, M.M., Stachenfeld, N.S., 2018. Sex differences in endothelial function important to vascular health and overall cardiovascular disease risk across the lifespan. Am. J. Physiol. Heart Circ. Physiol. https://doi.org/10.1152/ajpheart.00396.2018.
Stelmaszewska, J., Chrusciel, M., Doroszko, M., Akerfelt, M., Ponikwicka-Tyszko, D., Nees, M., Frentsch, M., Li, X., Kero, J., Huhtaniemi, I., Wolczynski, S., Rahman, N.A., 2016. Revisiting the expression and function of follicle-stimulation hormone receptor in human umbilical vein endothelial cells. Sci. Rep. https://doi.org/10.1038/srep37095.
Stilley, J.A., Guan, R., Duffy, D.M., Segaloff, D.L., 2014. Signaling through FSH receptors on human umbilical vein endothelial cells promotes angiogenesis. J. Clin. Endocrinol. Metab. https://doi.org/10.1210/jc.2013-3186.
Sun, H.J., Wu, Z.Y., Nie, X.W., Bian, J.S., 2020. Role of endothelial dysfunction in cardiovascular diseases: the link between inflammation and hydrogen sulfide. Front. Pharmacol. https://doi.org/10.3389/fphar.2019.01568.
Sun, L., Peng, Y., Sharrow, A.C., Iqbal, J., Zhang, Z., Papachristou, D.J., Zaidi, S., Zhu, L. L., Yaroslavskiy, B.B., Zhou, H., Zallone, A., Sairam, M.R., Kumar, T.R., Bo, W., Braun, J., Cardoso-Landa, L., Schaffler, M.B., Moonga, B.S., Blair, H.C., Zaidi, M., 2006. FSH directly regulates bone mass. Cell. https://doi.org/10.1016/j.cell.2006.01.051.
Tan, D., Zhao, Y., Ma, D., Tong, F., 2021. Role of FSH and FSH receptor on HUVECs migration. Gene Ther. https://doi.org/10.1038/s41434-020-00195-w.
Tedjawirja, V.N., Mieremet, A., Rombouts, K.B., Yap, C., Neele, A.E., Northoff, B.H., Chen, H.J., Vos, M., Klaver, D., Yeung, K.K., Balm, R., De Waard, V., 2023. Exploring the expression and potential function of follicle stimulating hormone receptor in extragonadal cells related to abdominal aortic aneurysm. PLoS One. https://doi.org/10.1371/journal.pone.0285607.
Widmer, R.J., Lerman, A., 2014. Endothelial dysfunction and cardiovascular disease. Glob. Cardiol. Sci. Pract. https://doi.org/10.5339/gcsp.2014.43.
Xiang, D., Liu, Y., Zhou, S., Zhou, E., Wang, Y., 2021. Protective effects of estrogen on cardiovascular disease mediated by oxidative stress. Oxid. Med. Cell. Longev. https://doi.org/10.1155/2021/5523516.
Zaidi, M., Lizneva, D., Kim, S.M., Sun, L., Iqbal, J., New, M.I., Rosen, C.J., Yuen, T., 2018. FSH, bone mass, body fat, and biological aging. Endocrinology. https://doi.org/10.1210/en.2018-00601.